CHIN. PHYS. LETT. Vol. 32, No. 4 (2015) 044101

# Doppler Spectrum Analysis of Time-Evolving Sea Surface Covered by Oil Spills *

YANG Peng-Ju(杨鹏举)[1**], GUO Li-Xin(郭立新)[1,2], JIA Chun-Gang(贾春刚)[1]

[1]*School of Physics and Optoelectronic Engineering, Xidian University, Xi'an 710071*

[2]*State Key Laboratory of Integrated Services Networks, Xidian University, Xi'an 710071*

(Received 29 July 2014)

*Based on the model of a contaminated sea surface that was proposed by Lombardini et al., the influence of the damping effect of oil films on the sea surface roughness spectrum and the geometrical structure of the sea surface is examined in detail by comparing with a clean sea surface. Furthermore, based on a quasi-stationary algorithm, a time series of backscattered echoes from a time-evolving sea surface covered by oil slicks is obtained by utilizing the frequency-domain numerical method of the parallel fast multiple method. Then, the Doppler spectrum is evaluated by performing a standard spectral estimation technique. Finally, the influence of the oil film damping effect on the Doppler spectrum of the backscattered echoes from time-evolving sea surface is investigated in detail by making a comparison of the Doppler spectrum of an oil-covered sea surface with the Doppler spectrum of a clean sea surface. The numerical simulations show that the damping effect of oil films has an influence on the Doppler spectrum signature for both horizontal-to-horizontal and vertical-to-vertical polarizations.*

*PACS:* 41.20.−q, 42.25.Bs, 42.25.Dd DOI: 10.1088/0256-307X/32/4/044101

Oil spills on the sea surface are observed relatively frequently and they represent a serious threat to the marine environment. However, the monitoring of oil spills on time-evolving sea surfaces is a challenging task,[1] due to the complexity of the ocean surface, together with the complexity of the electromagnetic (EM) scattering mechanism. The problem of remote sensing of oil spills on rough sea surfaces has been investigated experimentally and theoretically. Great research effort on this topic has been devoted to the analysis and processing of remote sensing data, particularly by synthetic aperture radars (SARs).[2,3] Furthermore, many researchers have presented quantitative electromagnetic modeling of sea oil spills on the sea surface,[4−6] which serves as the basis for remote sensing of oil spills on a rough ocean surface and actually involves the investigation on EM scattering from stratified rough surfaces,[7−10] which has attracted considerable attention due to its extensive applications in optics for coated surfaces, remote sensing of oil spills,[1] and the detection of buried interfaces. Compared with the normalized radar cross section (NRCS) of the sea surface, Doppler spectra of the backscattered echoes from time-evolving sea surface contains more information related to sea wave motion, and proves to be a much more precise and sensitive tool for monitoring fluid motion, which is of practical importance in many areas, such as sea surface wind retrieval, oceanic surface current measurement, and sea wave monitoring. Most of the literature on this topic is concentrated primarily on the Doppler spectra analysis of linear or nonlinear time-varying ocean surface.[11−14] However, to our knowledge, no research to date on Doppler spectra of the backscattered signals from time-evolving sea surface covered by oil slicks has been reported.

Consequently, the present study is devoted to an investigation on the Doppler spectra analysis of oil spills on time-evolving one dimensional (1D) dielectric sea surfaces, which is motivated by the fact that oil slicks damp the capillary wave components of the sea surface and thus change the geometrical structure of the sea surface,[4] which then exert an influence on the EM scattering features, as well as the Doppler spectra signature of the backscattered echoes.

The investigation on the Doppler spectra of backscattered echoes from oil-covered sea surfaces involves the calculation of EM scattering from a two-layered rough surfaces, as illustrated in Fig. 1. By applying Green's theorem to the three media divided by the two rough interfaces, respectively, one can derive the surface integral equations for calculating EM scattering from the one-dimensional two-layered dielectric rough surfaces in the three media, which are not presented here due to the space limitation and can be found in Ref. [15]. By applying pulse basis functions and points matching procedure to the integral equations, one can obtain a matrix equation, which can be solved by the parallel fast multiple method based on message-passing-interface (MPI) to accelerate the scattering calculations.[15] Upon solving the matrix equation the surface electric current and surface magnetic current can be obtained. The far-field can then be calculated by utilizing Huygens' principle.

Based on quasi-stationary algorithm,[11] a time series of backscattered echoes from a time-evolving sea surface covered by oil slicks can be obtained by utilizing the frequency-domain numerical method of the parallel fast multiple method. We will then conduct the Doppler spectra simulation and analysis of

*Supported by the National Science Foundation for Distinguished Young Scholars of China under Grant No 61225002, and the Aeronautical Science Fund and Aviation Key Laboratory of Science and Technology on AISSS of China under Grant No 20132081015.

**Corresponding author. Email: pjyang@yeah.net

© 2015 Chinese Physical Society and IOP Publishing Ltd

backscattered echoes from oil-covered sea surfaces in the following.

According to the model proposed by Lombardini *et al.*,[16] the roughness spectrum of an oil-covered sea surface $S_{\rm cont}$ is related to the clean sea surface roughness spectrum $S_{\rm clean}$ by the following ratio

$$S_{\rm cont}(k;u,E_0,\omega_{\rm D}) = \frac{S_{\rm clean}(k;u,E_0,\omega_{\rm D})}{y_{\rm s}(k;E_0,\omega_{\rm D})}, \quad (1)$$

where $y_{\rm s}$ is the damping ratio and $u$ is the wind speed. We only consider the insoluble films and a fully covered sea, and thus the damping ratio $y_{\rm s}$ is expressed by

$$y_{\rm s}(f,E_0,\omega_{\rm D}) = \frac{1-2\tau+2\tau^2-X+Y(X+\tau)}{1-2\tau+2\tau^2-2X+2X^2}, \quad (2)$$

where

$$\tau = \left(\frac{\omega_{\rm D}}{2\omega}\right)^{\frac{1}{2}},\ X = \frac{E_0k^2}{\rho(2\nu\omega^3)^{0.5}},\ Y = \frac{E_0k}{4\rho\nu\omega} \quad (3)$$

are dimensionless quantities, and

$$f = \frac{\omega}{2\pi} = \frac{(\varsigma k^3/\rho+gk)^{1/2}}{2\pi} \quad (4)$$

is the dispersion law. In Eqs. (2)–(4), $\rho$ is the water density, $g$ is the acceleration of gravity, $\nu = 10^{-6}\,{\rm m/s}$ is the kinematic viscosity, $\varsigma = 74\times10^{-3}\,{\rm N/m}$ is the surface tension, $E_0$ denotes the elasticity modulus, and $\omega_{\rm D}$ represents a characteristic pulsation. This study considers two different types of oil films with parameters $\{\omega_{\rm D} = 6.0\,{\rm rad/s},\ E_0 = 9\,{\rm mN/m}\}$ and $\{\omega_{\rm D} = 11.0\,{\rm rad/s},\ E_0 = 25\,{\rm mN/m}\}$. It is necessary to note that these values were retrieved from experiments conducted in the Sicilian channel and the gulf of Maine.[16]

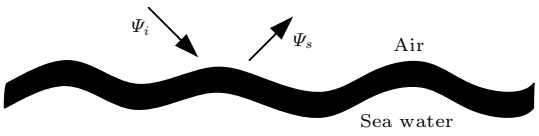



**Fig. 1.** Geometry of a 1D rough sea surface covered by an oil film.

In this work, the contaminated and clean sea surfaces are generated as realizations of a Gaussian random process with the roughness spectrum of an oil-covered sea surface $S_{\rm cont}$ and the clean sea surface roughness spectrum $S_{\rm clean}$ of the Pierson–Moskowitz spectrum,[17] respectively, which is expressed as

$$S(k) = \frac{\alpha}{4|k|^3}\exp\left(-\frac{\beta g^2}{k^2U_{19.5}^2}\right), \quad (5)$$

where $k$ is the spatial wave number defined for both positive and negative values, $\alpha = 8.10\times10^{-3}$, $\beta = 0.74$, $g = 9.81\,{\rm m/s^2}$ is the acceleration of gravity, and $U_{19.5}$ is the wind speed at a height of 19.5 m.

The Doppler spectrum is defined as the power spectral density of the random time-varying scattering amplitude and can be evaluated by utilizing a standard spectral estimation technique in terms of the following expression[11]

$$S(f) = \left\langle \frac{1}{T}\left|\int_0^T \psi_{\rm s}(t,\theta_{\rm s},\theta_{\rm i})e^{-i2\pi ft}\right|^2\right\rangle, \quad (6)$$

where the angular bracket represents the ensemble average over random surface realizations and $\psi_{\rm s}(t,\theta_{\rm s},\theta_{\rm i})$ denotes the scattered field. In Eq. (6), $\theta_{\rm i}$ is the incidence angle, $\theta_{\rm s}$ is the scattering angle, $t$ is the time, $T$ is the sea surface evolution time, $f$ denotes the frequency in frequency domain of Fourier transformation, and $S(f)$ represents the Fourier spectrum of the scattered field time series $\psi_{\rm s}(t,\theta_{\rm s},\theta_{\rm i})$. In the following, we consider only the backscattering case, i.e., $\theta_{\rm s} = -\theta_{\rm i}$.

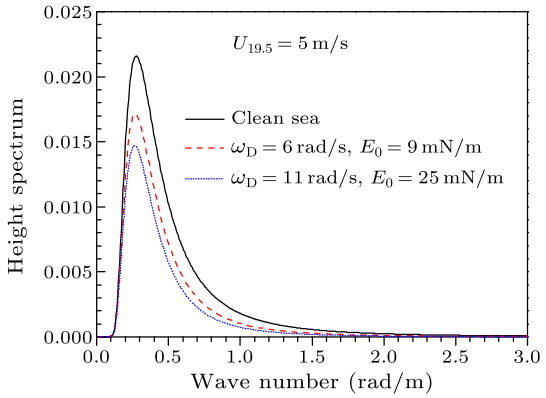



**Fig. 2.** Height spectra of clean and oil-covered sea surface versus the wavenumber $k$ with wind speed $U_{19.5} = 5\,{\rm m/s}$.

To quantitatively measure the Doppler spectrum, the Doppler shift $f_{\rm c}$, i.e. the spectral centroid, and the bandwidth of the Doppler spectrum $f_{\rm w}$ can be defined by

$$f_{\rm c} = \frac{\int fS(f)df}{\int S(f)df},$$
$$f_{\rm w} = \sqrt{\frac{\int (f-f_{\rm c})^2S(f)df}{\int S(f)df}}. \quad (7)$$

The Doppler shift $f_{\rm c}$, which is an important parameter of the Doppler spectrum, corresponds to a power-weighted mean line-of-sight velocity of the scatterers. However, the bandwidth of the Doppler spectrum $f_{\rm w}$ is determined by the variance of the velocity distribution of the scattering facets at the sea surface. In this work, however, the Doppler shift $f_{\rm c}$ and the bandwidth of the Doppler spectrum $f_{\rm w}$ are not presented due to the space limitation.

Figure 2 presents the influence of the oil film on the roughness spectra of the rough sea surface with the wind speed $U_{19.5} = 5.0\,{\rm m/s}$. It is observed that the higher wave number components corresponding to shorter waves of the sea surface roughness spectrum are significantly influenced by the oil film, whereas the lower wave number components corresponding to longer waves of the sea surface roughness spectrum are

slightly influenced by the oil film. More precisely, the magnitude of the contaminated sea roughness spectrum is smaller than that of the clean sea roughness spectrum for shorter waves. Moreover, the magnitude of the contaminated sea roughness spectrum with oil film parameters $\{\omega_D = 11\,\text{rad/s},\ E_0 = 25\,\text{mN/m}\}$ is smaller than that of the contaminated sea roughness spectrum with oil film parameters $\{\omega_D = 6\,\text{rad/s},\ E_0 = 9\,\text{mN/m}\}$ for shorter waves. This can be attributed to the fact that the oil film strongly damps the higher frequency components of the sea surface and have a slight impact on lower frequency components of the sea surface, and that the contaminated sea with oil film parameters $\{\omega_D = 11\,\text{rad/s},\ E_0 = 25\,\text{mN/m}\}$ has a stronger damping effect than the oil-covered sea with parameters $\{\omega_D = 6\,\text{rad/s},\ E_0 = 9\,\text{mN/m}\}$ for the shorter waves of the sea surface. This damping effect will then influence the geometrical structure of the sea surface, as well as the statistical characteristics, which will be discussed in detail in the following.

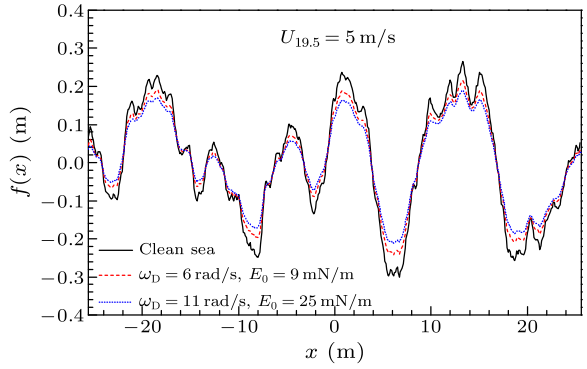



**Fig. 3.** Comparison of the sea surface height profile between a clean sea surface and an oil-covered sea.

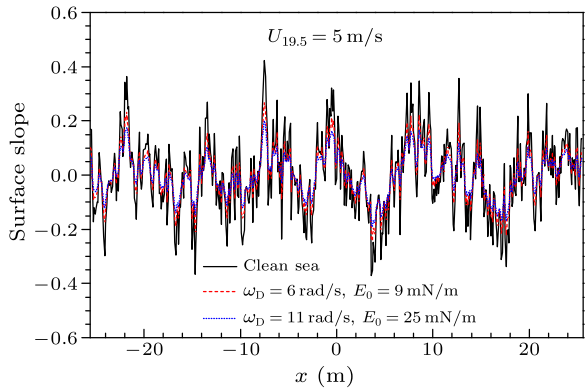



**Fig. 4.** Comparison of the sea surface slope between a clean sea surface and an oil-covered sea.

The surface height and surface slope of a realization of clean sea surface and two different types of contaminated sea with parameters $\{\omega_D = 6\,\text{rad/s},\ E_0 = 9\,\text{mN/m}\}$ and $\{\omega_D = 11\,\text{rad/s},\ E_0 = 25\,\text{mN/m}\}$ are plotted in Figs. 3 and 4, respectively. It is readily observed that both the surface height and the surface slope of a contaminated sea have a smaller magnitude compared with that of a clean sea surface, and surface height and surface slope of an oil-covered sea with parameters $\{\omega_D = 11\,\text{rad/s},\ E_0 = 25\,\text{mN/m}\}$ are smaller than that with parameters $\{\omega_D = 6\,\text{rad/s},\ E_0 = 9\,\text{mN/m}\}$. It is also found that the contaminated sea surface heights are somewhat smaller than those of a clean sea surface in Fig. 3, whereas the slopes of the contaminated sea are much smaller than those of a clean sea surface, as depicted in Fig. 4.

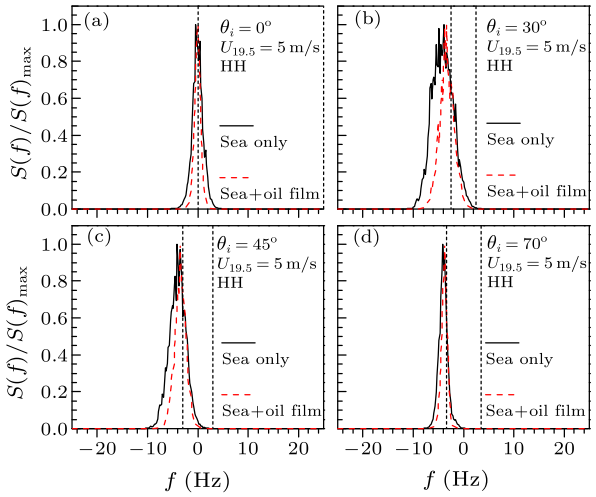



**Fig. 5.** Comparison of the normalized Doppler spectra of backscattered echoes from a clean and a contaminated sea surface (horizontal polarization).

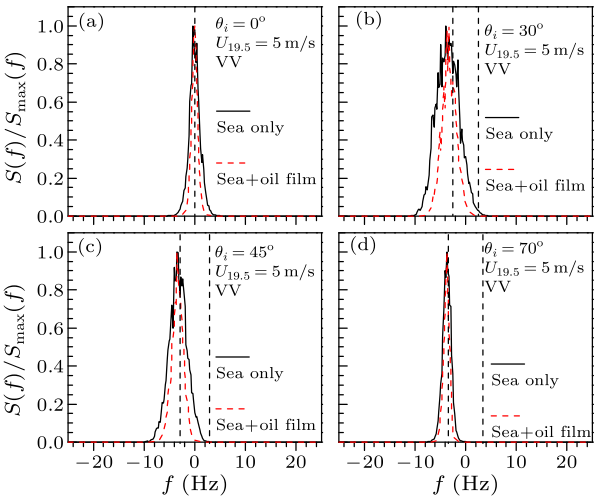



**Fig. 6.** Comparison of the normalized Doppler spectra of backscattered echoes from a clean and a contaminated sea surface (vertical polarization).

We attribute this phenomenon to the fact that both the surface height and the surface slope are damped by the oil film, and the damping effect is stronger for oil films with parameters $\{\omega_D = 11\,\text{rad/s},\ E_0 = 25\,\text{mN/m}\}$ than for oil films with parameters $\{\omega_D = 6\,\text{rad/s},\ E_0 = 9\,\text{mN/m}\}$. Moreover, the surface slope is more strongly damped compared with the surface height.

In this work, the numerical simulations are performed at a frequency of $f = 1.2\,\text{GHz}$ with the corresponding electromagnetic wavelength $\lambda = 0.25\,\text{m}$. At $f = 1.2\,\text{GHz}$, the relative permittivity of sea surface

is $\varepsilon_r = 73.2 + i67.2$ at sea water temperature of 20℃ and salinity of 30 parts per thousand in terms of Debye expression,[18] and the relative permittivity of the oil film is taken as $\varepsilon_r = 2.25 + i0.01$.[19] An insoluble homogeneous film is assumed in this work with parameters $\{\omega_D = 11\,\text{rad/s},\ E_0 = 25\,\text{mN/m}\}$ and mean thickness of $0.1\lambda$. The Pierson–Moskowitz spectrum is utilized as the clean sea surface roughness spectrum with wind speed $U_{19.5} = 5\,\text{m/s}$ at a height of 19.5 m. The length of the sea surface is $L = 102.4\lambda$, and the Thorsos tapered plane wave[20] with tapering parameter $g = L/6$ is chosen as the incident field to reduce the edge diffraction effect due to the truncation of a rough surface. For a Doppler spectra simulation, the criterion that is used to choose the time interval is discussed in detail in Ref. [11]. In the following simulation, the time step is set to 0.02 s to obtain sufficient unambiguous Doppler bandwidth, and each realization of Doppler spectrum is preformed on 256 time samples to obtain sufficient Doppler spectral resolution. The final average Doppler spectra are obtained over 100 ensemble realizations.

Figures 5 and 6 exhibit a comparison of the normalized Doppler spectra of backscattered echoes from the clean sea surface and the contaminated sea surface with wind speed $U_{19.5} = 5\,\text{m/s}$ for the horizontal polarization and the vertical polarization, respectively. It should be mentioned that the amplitudes of the Doppler spectra of the oil-covered sea surface are actually smaller than that of the oil-free sea surface for larger incidence angles arising from the absorption of the oil film, which are not presented here due to the space limitation. Thus, the Doppler spectra of clean sea and contaminated sea are normalized to their respective maximum values to compare the Doppler shift and bandwidth of the Doppler spectrum.

The Bragg shift is also plotted with vertical dashed lines, which is predicted by small perturbation method (SPM) at first order and is expressed by $f_B = \pm\sqrt{gK_B \sin\theta_i}/2\pi$ with $K_B(\theta_i) = 2k_0 \sin(\theta_i)$ being the Bragg wavenumber.[21] It is observed that the bandwidth of the Doppler spectrum of the oil-covered sea is smaller than that of an oil-free sea for both horizontal-horizontal (HH, horizontal for receiving antenna and horizontal for transmitting antenna) and vertical-vertical (VV) polarizations, especially for moderate incidence angles. It is also observed that the Doppler spectra of the oil-free sea surface are shifted to higher frequencies compared with that of the oil-covered sea surface. This can be attributed to the fact that the oil-covered sea has a relative small surface height and surface slope due to the damping effect of the oil film, which consequently makes the oil-covered sea surface much smoother compared with the oil-free sea surface. As the incidence angle increases, the Doppler spectra of clean sea and contaminated sea for both HH and VV polarizations first become broader and then shrink. Similar results for a clean sea have been reported in Ref. [11]. It is found that the Doppler shifts of clean sea and contaminated sea for both HH and VV polarizations are close to the Bragg shift for small incidence angles and are near low grazing angles, whereas the Doppler shift departs from the Bragg shift for moderate incidence angles.

In conclusion, the influence of the damping effect of oil films on the sea surface roughness spectrum and the geometrical structure of the sea surface is examined by comparing it with those of a clean sea surface, which shows that the damping effect changes the geometrical structure of the sea surface and actually reduces the height and slope of the sea surface. Meanwhile, the influence of oil film on the Doppler spectrum signature is investigated by comparison of the Doppler spectrum of an oil-covered sea surface with the Doppler spectrum of a clean sea surface. The numerical simulations show that the bandwidth of the Doppler spectrum of the oil-covered sea is smaller than that of an oil-free sea for both HH and VV polarizations, especially for moderate incidence angles, and that the Doppler spectra of the oil-free sea surface are shifted to higher frequencies compared with the oil-covered sea surface. This can be attributed to the fact that an oil-covered sea has a relative small surface height and surface slope due to the damping effect of the oil film, which consequently makes the oil-covered sea surface much smoother compared with the oil-free sea surface.

## References


[1] Solberg A H S 2012 *Proc. IEEE* **100** 2931
[2] Nunziata F, Gambardella A and Migliaccio M 2008 *IEEE Geosci. Remote Sens. Lett.* **5** 691
[3] Salberg A B, Rudjord O and Solberg A H S 2014 *IEEE Trans. Geosci. Remote Sens.* **52** 6521
[4] Pinel N, Déchamps N and Bourlier C 2008 *IEEE Trans. Geosci. Remote Sens.* **46** 385
[5] Wang R, Guo L X, Wang A Q and Wu Z S 2011 *Chin. Phys. Lett.* **28** 034101
[6] Pinel N, Bourlier C and Sergievskaya I 2014 *IEEE Trans. Geosci. Remote Sens.* **52** 2326
[7] Li J, Guo L X and Zeng H 2009 *Chin. Phys. Lett.* **26** 034101
[8] Demir M A, Johnson J T and Zajdel T J 2012 *IEEE Trans. Geosci. Remote Sens.* **50** 3374
[9] Duan X Y and Moghaddam M 2013 *IEEE Trans. Geosci. Remote Sens.* **51** 2722
[10] Pinel N, Johnson J T and Bourlier C 2010 *IEEE Trans. Antennas Propag.* **58** 809
[11] Toporkov J V and Brown G S 2000 *IEEE Trans. Geosci. Remote Sens.* **38** 1616
[12] Johnson J T, Toporkov J V and Brown G S 2001 *IEEE Trans. Geosci. Remote Sens.* **39** 2411
[13] Wang Y H, Zhang Y M and Guo L X 2010 *Chin. Phys. Lett.* **27** 104101
[14] Miret D, Soriano G, Nouguier F, Forget P, Saillard M and Guérin C A 2014 *IEEE Trans. Geosci. Remote Sens.* **52** 7120
[15] Guo L X, Wang A Q and Chai C 2011 *IET Microwaves Antennas Propag.* **5** 1813
[16] Lombardini P, Fiscella B, Trivero P, Cappa C and Garrett W 1989 *J. Atmos. Oceanic Technol.* **6** 882
[17] Thorsos E I 1990 *J. Acoust. Soc. Am.* **88** 335
[18] Stogryn A 1971 *IEEE Trans. Microwave Theory Tech.* **19** 733
[19] Folgerø K 1996 *Meas. Sci. Technol.* **7** 1260
[20] Thorsos E I 1988 *J. Acoust. Soc. Am.* **83** 78
[21] Bass F G, Fuks I M, Kalmykov A I, Ostrovsky I E and Rosenberg A D 1968 *IEEE Trans. Antennas Propag.* **16** 554